

## JET-GAS INTERACTIONS IN THE SEYFERT GALAXY MARKARIAN 78

M. Whittle,<sup>1</sup> A. S. Wilson,<sup>2</sup> C. H. Nelson,<sup>3</sup> D. Rosario,<sup>1</sup> and J. D. Silverman<sup>1,4</sup>

### RESUMEN

La galaxia Markarian 78 de tipo Seyfert 2 ofrece la escasa oportunidad de estudiar la interacción de flujos de radio en escalas de kpc con el gas emisor de líneas que lo rodea. Usando imágenes y espectroscopía de VLA y de *HST* identificamos varias signaturas de la interacción, incluyendo interrupción y deflexión del jet. Usando las características cinemáticas identificamos tres regiones que muestran estados iniciales, intermedios y avanzados de desbaratamiento de nubes por el flujo del jet. Las razones de las líneas espectrales no favorecen exclusivamente ionización ya sea por fotones o por choques. Sin embargo, las correlaciones entre las razones de las líneas y las velocidades dan argumentos contra la importancia de la ionización por choques.

### ABSTRACT

The Seyfert 2 galaxy Markarian 78 offers a rare opportunity to study the interaction of kpc scale radio outflows with the surrounding emission line gas. Using VLA and *HST* imaging and spectroscopy we identify a number of signatures of the interaction, including jet disruption and deflection. Folding in kinematic features, we identify three regions which may be exhibiting early, intermediate, and late stages of cloud disruption by the jet flow. Emission line ratios do not uniquely favour either photo- or shock ionization, however the lack of correlations between line ratios and velocities argues against the importance of shock ionization.

*Key Words:* **GALAXIES: INDIVIDUAL (MARKARIAN 78) — GALAXIES: ISM — GALAXIES: JETS — GALAXIES: SEYFERT**

### 1. INTRODUCTION

Seyferts provide an important window on jet-gas interactions—jets of intermediate power and scale enter a gas rich environment. The jets are traceable, at least in part, by radio synchrotron emission which provides useful information not only on geometry but also on pressures and energies. The ionized gas in the near nuclear regions of Seyferts yields a strong emission line spectrum which in turn provides powerful kinematic, ionization and physical diagnostics. Set against these positive qualities are some difficulties. Seyfert emission line regions are rarely larger than a few arcseconds, and the jet-gas interactions are only one of several possible ongoing processes. For example, in most objects most of the gas is in gravitational motion, while central source photoionization at least contributes and usually dominates the ionization of the gas. For these and other reasons, good examples to study jet-gas interactions are quite difficult to find, despite the impression one gets from most papers or talks which, of course, focus on the minority of objects with prominent jets.

Markarian 78 was the most promising object to emerge from a ground-based survey of Seyferts with

linear radio sources larger than 0.75 arcsecs in extent (Whittle et al. 1988). It has a relatively large triple radio source  $\sim 4$  arcsecs in extent, which is aligned and cospatial with the [O III] emission. Long slit spectroscopy suggested jet driven super-virial motions. Thus, Mkn 78 is a good target for an intensive *HST*/VLA study. One potential limitation—Mkn 78 has higher redshift than many other Seyferts studied in detail, so that 0.1 arcsec resolution corresponds to  $\sim 70$  pc ( $cz = 11,000$  km s<sup>-1</sup>;  $H_0 = 75$  km s<sup>-1</sup> Mpc<sup>-1</sup>).

Early ground based work includes continuum and emission line imaging (Haniff, Wilson, & Ward 1988); and long slit spectroscopy (Whittle et al. 1988; Pedlar et al. 1989), while previous *HST* studies include those of Capetti et al. (1994, 1996).

### 2. OBSERVATIONS

Our data set includes a relatively deep 8-hr VLA integration at 3.6cm giving comparable resolution to *HST*; *HST* images in *V* and *U* continuum, [O III] and [O II] emission lines; and two spectroscopic programs—an FOS program of 10 apertures of 0.43 arcsec diameter and a STIS program of 4 slits. In both spectroscopic programs our aim was to cover important diagnostic lines in both the optical and UV as well as to obtain higher resolution in the [O III] region to map the kinematics.

<sup>1</sup>University of Virginia, USA.

<sup>2</sup>University of Maryland, USA.

<sup>3</sup>University of Nevada, USA.

<sup>4</sup>Center for Astrophysics, Harvard, USA.

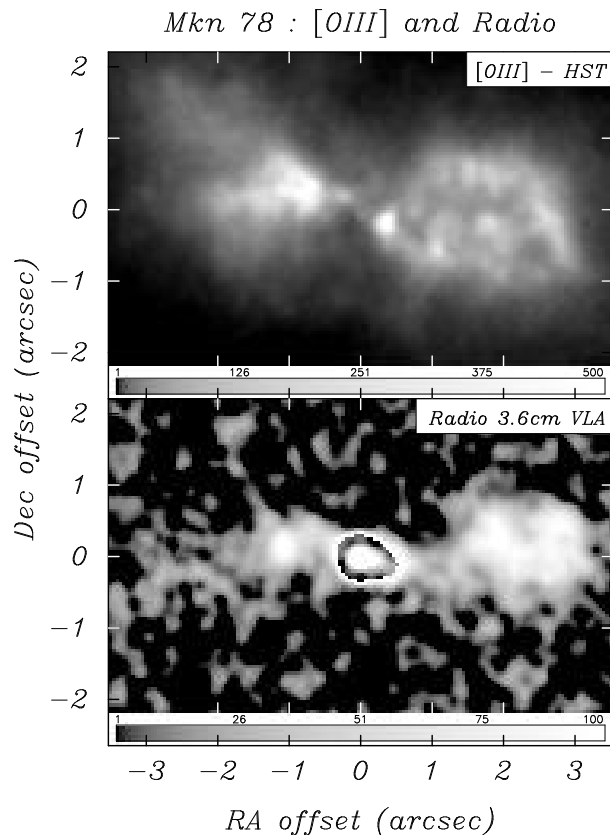


Fig. 1. *HST* [O III] emission line image and VLA radio image of the Seyfert 2 galaxy Mkn 78. Note that a dust lane crosses the nucleus hiding the most nuclear [O III] emission. Grey scale numbers are proportional to flux, with the radio core rescaled by a factor five for clarity.

### 3. MORPHOLOGY

We begin by describing the morphology of the radio and [O III] images, before turning to the kinematic state of the gas and then its ionization state.

Figure 1 shows the 3.6-cm radio structure. Note the bright core which includes an inner bent jet-like feature which terminates  $\sim 0.5$  arcsec from the nucleus. Emission to the east appears to undergo a bend while emission to the west comprises a radio lobe with some substructures. Fig. 1 also shows the [O III] image to the same scale. A dust lane obscures the nuclear regions; emission to the east comprises a higher surface brightness, inner ‘fan’ at the apex of a larger, lower surface brightness, outer fan; while the western emission comprises a number of knots including a bright compact knot  $\sim 0.5$  arcsec west of the nucleus.

Figure 2 shows the superposition of the radio (contours) and [O III] (grayscale) images. Here we draw attention to four morphological features:

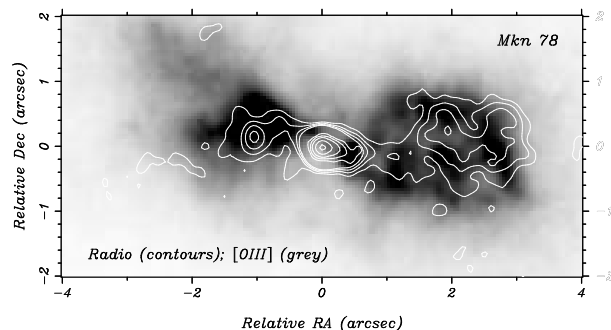


Fig. 2. Radio contours superposed on the [O III] image. For the central emission, the naturally weighted higher resolution radio data has been used. Examples of radio source termination, deflection and interaction are evident.

1. The inner radio jet terminates and spreads at the inner western [O III] knot, leading us to expect strong signatures of jet-gas interaction.

2. The eastern radio emission appears to be deflected right at the front of the inner [O III] fan, and continues along the edge of the fan. The shape of the fan may itself arise in part due to this dynamical interaction.

3. The relation between western components is more complex, with no obvious correspondence, and indeed there is some tendency for the radio sub-peaks to lie between the [O III] sub-peaks, as found in the lobe emission in some other Seyferts (e.g., Falcke, Wilson, & Simpson 1998) and low-redshift radio galaxies (e.g., van Breugel et al. 1984a,b).

4. Finally, there is evidence of central source illumination in the [O III] image, particularly at low flux levels—the eastern fan, the inner boundary of the western lobe, and the outer western ENLR (not shown).

### 4. KINEMATICS

Turning now to the kinematics, Figure 3 shows the STIS data on the [O III]  $\lambda 5007$  line for the four slits. Note that with data from other lines, we are not only able to monitor the gas velocity and linewidth along each slit, but also the line flux, reddening corrections, electron density and, using all these, the projected distributions of momentum and kinetic energy. We note several features in these kinematic plots:

(a) There is little disturbance of the inner western knot, despite the fact that the radio jet is disrupted at this point and we expected strong signs of jet-gas interaction. This suggests a fairly low limit to the contribution of shock ionized gas (as opposed to pre-cursor ionized gas) in this feature.

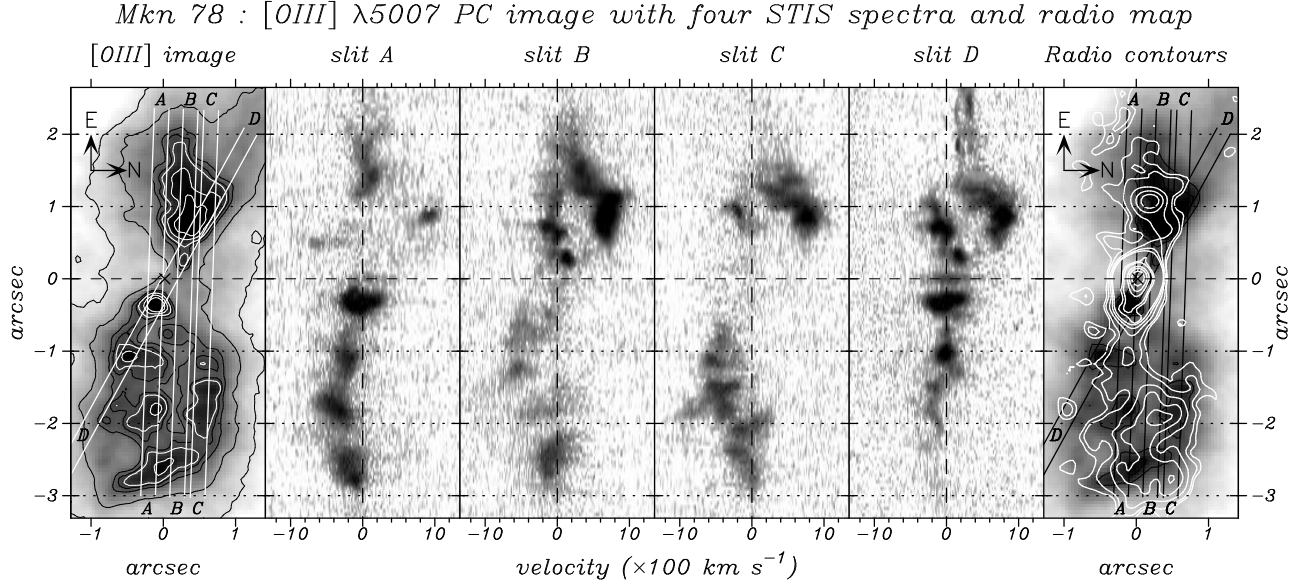


Fig. 3. [O III]  $\lambda 5007$  emission line from four STIS slits crossing the NLR. The velocity scale indicates projected speeds of up to  $\pm 1000 \text{ km s}^{-1}$ .

(b) Over the eastern fan, the lines are split by  $\sim 700 \text{ km s}^{-1}$ . One interpretation is that the jet is driving gas laterally, giving both red and blue shifted components at the same projected location. Additional evidence for jet interaction at this point is a sharp increase in the gas density (derived from the [SII]  $\lambda 6717, 6731$  lines) close to the location of the jet deflection. Note also that at this location the jet is deflected not disrupted, with the cloud providing sufficient inertia to redirect the jet flow.

(c) Immediately beyond the radio source on the eastern side, the gas velocities begin to drop back to the galactic rotation value. Clearly, in the absence of ongoing acceleration, drag forces are important and relatively rapidly drain the gas of its kinetic energy and momentum.

(d) In the western lobe, the various knot velocities are more complex, with a general increase to  $\sim -500 \text{ km s}^{-1}$  at the lobe center. Rather than exhibiting a simple bow shock form, the western lobe resembles more chaotic acceleration within a “leaky bubble”.

A somewhat speculative scenario places these regions into a possible time sequence for a jet-cloud interaction. An early stage is seen in the inner west knot, where the initial impact disrupts the jet and has not yet had time to significantly influence the cloud. A later stage is seen at the eastern fan, where the jet has begun to disrupt and disperse the cloud, driving a lateral expansion and being deflected in the process. The outer western knots represent an even

later stage, where the jet flow has become decollimated while continuing to break up the cloud into separate knots. It is possible that an even later stage is seen in the Extended Narrow Line Region (ENLR; not shown in figures) which is a quiescent region of ionized gas at larger radii to the west, and may be a relic of a formerly disrupted cloud.

## 5. LINE RATIOS

Turning now to the emission line ratios, we make use principally of the FOS data at this time. Following earlier work (e.g., Binette, Wilson, & Storchi-Bergmann 1996; Dopita & Sutherland 1995, DS) we compare line ratios to predictions from three model sequences: optically thick photoionization models ( $U$ ); a varying mixture of optically thick and thin photoionized gas ( $A_{m/i}$ ); and a range of velocities for autoionizing shocks (Shocks) (see Figure 4 for a few examples). Briefly, all models reproduce satisfactorily the classic excitation ratios (e.g., [O III]/ $H\beta$ , [O III]/[O II], [Ne III]/[O II]) giving  $\log U = -2.64 \pm 0.2$ ;  $\log A_{m/i} = 0.3 \pm 0.3$ ;  $V_{sh} = 400 \pm 100 \text{ km s}^{-1}$ . For the low ionization lines (e.g., [O I], [N II], [S II]) shocks are a poor fit to the ratios, overpredicting [O I] by a factor  $\sim 2.5$  (the published models of DS overestimate [O I] and [N I] by a factor 4; Dopita 2000), while the [N II]/ $H\alpha$  versus [O III]/[N II] data nicely follow the  $U$  and  $A_{m/i}$  sequences but fall away from the shock sequence. The classic model discriminators complicate the picture. The [O III]  $\lambda 4363$  line is fit worse by the  $U$  sequence, better by the shock sequence and best by the  $A_{m/i}$  sequence. Thus, while

Emission Lines from Jet Flows (Isla Mujeres, Q.R., México, November 13-17, 2000)  
Editors: W. J. Henney, W. Steffen, A. C. Raga, & L. Binette

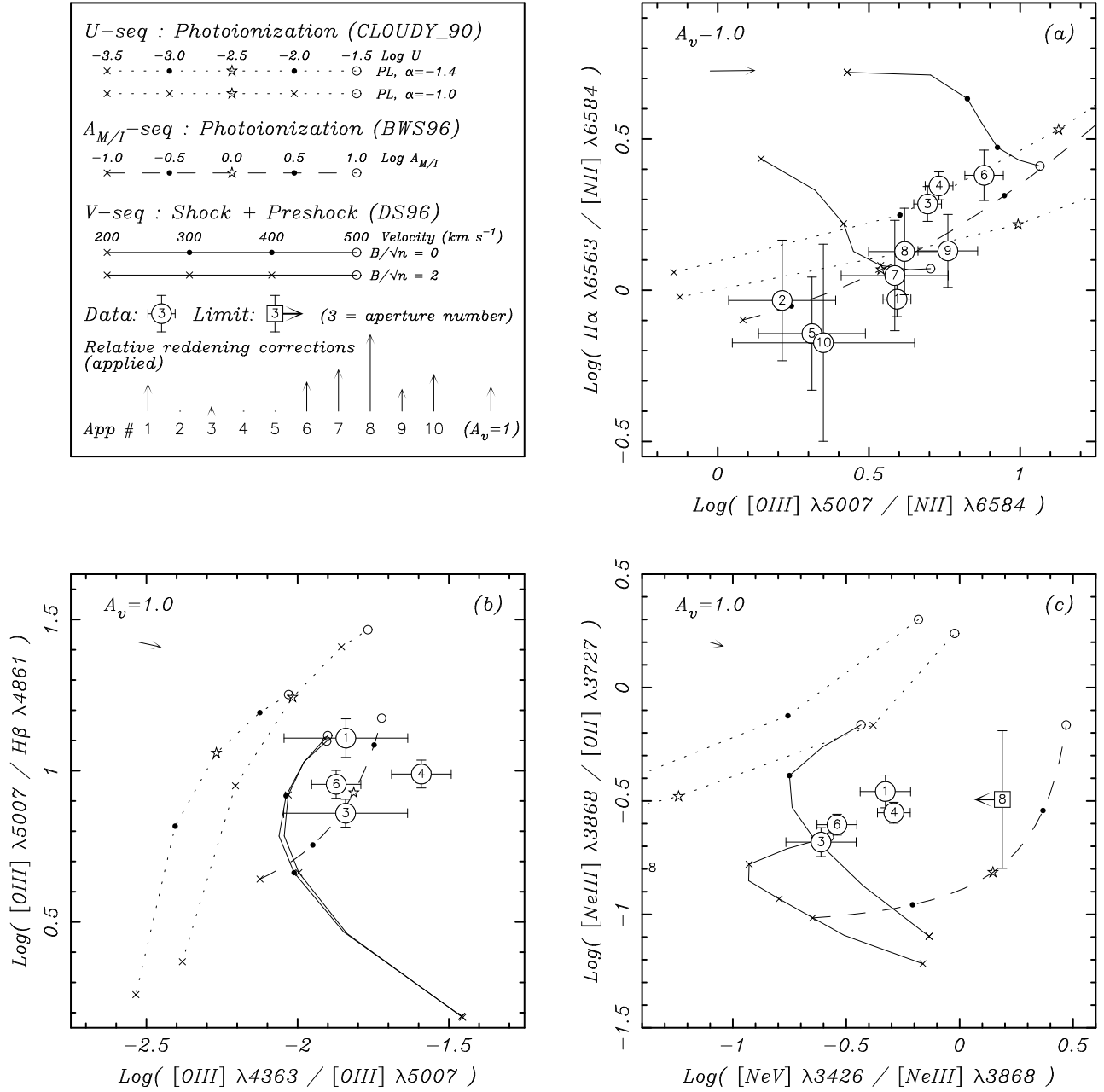


Fig. 4. Several important line ratios from FOS spectra plotted against various model calculations (identified in the top left panel).

the  $U$  models suffer the well-known ‘[O III] Temperature Problem’ (Tadhunter, Robinson, & Morganti 1989), the Shock and  $A_{m/i}$  sequences achieve higher temperatures, as they were designed to do. Although the He II  $\lambda 4686$  line has the potential to separate the  $U$  and  $A_{m/i}$  sequences, in the case of Mkn 78 it does not, fitting all models equally well. The last discriminator is the [Ne V]  $\lambda 3426$  line which is fit best by the

shock models and less well by the  $U$  and  $A_{m/i}$  models (though in opposite senses for each: too strong for  $U$  but too weak for  $A_{m/i}$ ). However, [Ne V] is unusually weak in Mkn 78 (by a factor  $\sim 3$  relative to other Seyferts) so it is unclear how to interpret this last result.

Overall, the simple comparison between observed line ratios and model predictions is rather inconclu-

sive. At face value, it seems that the shock models fit worst, with the  $U$  and  $A_{m/i}$  fit better, with the  $A_{m/i}$  fitting best.

Perhaps a more revealing approach is to look for correlations between line ratios and other properties, such as gas kinematics, local continuum color, or location in the region. Shock models predict at least some links between line ratios and kinematic parameters, such as FWHM,  $V - V_{\text{sys}}$ , or the quadrature sum of these two. Interestingly, as Figure 5 illustrates, no such relations exist—the highest velocity gas and the lowest velocity gas have approximately the same spectrum, while shock models predict significant differences, even if one allows for a mix of quiescent photoionized precursor gas as well as the accelerated post shock gas. This null result poses a serious problem for the shock models.

If the NLR gas is ionized by a locally produced continuum, one might expect correlations between excitation and local continuum color or UV excess. Possible sources of such a continuum might be shocks and/or star formation. There is some evidence for a weak trend such that bluer regions have higher excitation. If the blue continuum arises from recent star formation (as indicated from the presence of Balmer absorption lines), the link to the ionized gas must, of course, be indirect since the line ratios are certainly not those of H II regions. It is possible, for example, that gas associated with star formation is itself ionized by the central source. Another possibility is that the blue continuum comes from post shock gas. Arguing against this is the absence of correlation between kinematics and ionization, as well as the fact that the expected emission line equivalent widths would be much greater than they are observed to be.

There is also some tendency for emission away from the radio axis or farther from the nucleus to have somewhat lower excitation (with some exceptions). This would be consistent with ionization by the central (and partially obscured) nuclear radiation field.

## 6. SUMMARY

The morphological and kinematic data suggest that there is a strong interaction between the radio source and the ionized line emitting gas in Mkn 78—each significantly affects the other. The interaction not only affects the distribution of the ionized gas (and radio plasma) but also its velocity field.

It is possible to divide the emission into three somewhat distinct regions: the compact but kinematically quiet inner western [O III] knot lying at the

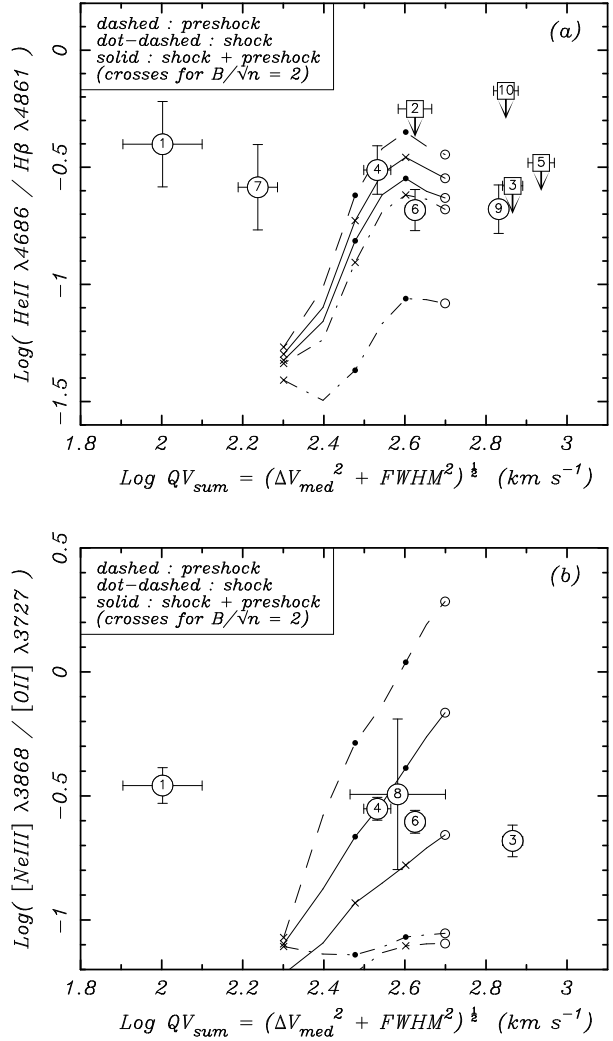


Fig. 5. Emission line ratios show no correlation with kinematic state of the gas. Here,  $QV_{\text{sum}}$  is the quadrature sum of the velocity offset from systemic ( $\Delta V_{\text{med}}$ ) and the local velocity spread (FWHM).

end of the inner radio jet; the kinematically highly disturbed eastern [O III] fan located near the bend in the eastern radio source; and the more dispersed western [O III] knots mingled with the outer radio components. These three regions suggest a possible temporal sequence for the interaction of the radio source with ISM clouds—an initial interaction disrupts the jet flow but takes time to influence the line emitting cloud (inner western knot); as time passes the jet begins to disrupt and accelerate the cloud (eastern fan); the cloud is finally dispersed into a number of knots by the jet flow which itself becomes decollimated (western knots). It is possible that the extended ENLR represents a yet later stage in this sequence.

Despite strong kinematic signatures, it is unclear if shocks dominate the ionization. The emission geometry at low flux levels suggests central source illumination; line ratios are fit worst by shock models compared to power law photoionization models; there is a notable absence of links between line ratios and the kinematic state of the gas.

We are very grateful to Luc Binette and Alex Raga for organising this conference. This work has been supported by NASA grants GO-5471 and GO-7404.

#### REFERENCES

- Binette, L., Wilson, A. S., & Storchi-Bergmann, T. 1994, *A&A* 312, 365
- Capetti, A., Axon, D. J., Macchetto, F., Sparks, W. B., & Boksenberg, A. 1996, *ApJ*, 469, 554
- Capetti, A., Macchetto, F., Sparks, W. B., & Boksenberg, A. 1994, *ApJ*, 421, 87
- Dopita, M. A. 2000, *Ap&SS*, 272, 79
- Dopita, M. A., & Sutherland, R. S. 1995, (DS), *ApJ*, 455, 468
- Falcke, H., Wilson, A. S., & Simpson, C. 1998, *ApJ*, 502, 199
- Haniff, C. A., Wilson, A. S., & Ward, M. J. 1988, *ApJ*, 334, 104
- Pedlar, A., et al. 1989, *MNRAS*, 238, 863
- Tadhunter, C. N., Robinson, A., & Morganti, R. 1989, in *Extranuclear Activity in Galaxies*, eds E. J. A. Meurs & R. A. E. Fosbury, *ESO Conf. and Workshop Proc. No. 32*, Garching, p. 293
- van Breugel, W. J. M., Heckman, T. M., Butcher, H. R., & Miley, G. K. 1984b, *ApJ*, 277, 82
- van Breugel, W. J. M., Heckman, T. M., & Miley, G. K. 1984a, *ApJ*, 276, 79
- Whittle, M., Pedlar, A., Meurs, E. J. A., Unger, S. W., Axon, D. J., & Ward, M. J. 1988, *ApJ*, 326, 125

Mark Whittle and David Rosario: Astronomy Department, University of Virginia, Charlottesville, VA 22903, (dmw8f,djr4t@virginia.edu).

Andrew Wilson: Astronomy Department, University of Maryland, College Park, MD 20742, (wilson@astro.umd.edu).

Charles Nelson: Physics Department, University of Nevada, Las Vegas, 4505 Maryland Parkway, Box 4002, Las Vegas, NV 89154-4002, (cnelson@physics.unlv.edu).

John Silverman: Center for Astrophysics, 60 Garden Street, Cambridge, MA 02138, (jds@head-cfa.harvard.edu).